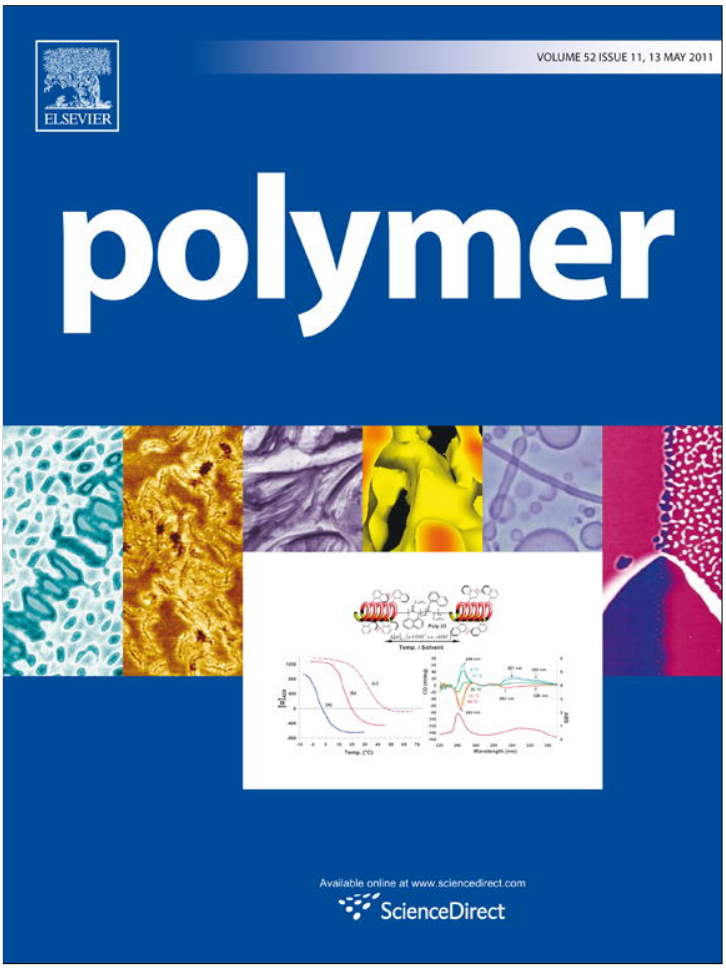

Polymer 52 (2011) 2445–2452

Contents lists available at ScienceDirect

Polymer

journal homepage: www.elsevier.com/locate/polymer

Molecular modeling of crosslinked epoxy polymers: The effect of crosslink density on thermomechanical properties

Ananyo Bandyopadhyay [a], Pavan K. Valavala [b], Thomas C. Clancy [c], Kristopher E. Wise [d], Gregory M. Odegard [a,*]

[a] Michigan Technological University, 1400 Townsend Drive, Houghton, MI 49931-1295, USA
[b] Northwestern University, 633 Clark Street Evanston, IL 60208, USA
[c] National Institute of Aerospace, 100 Exploration Way, Hampton, VA 23666, USA
[d] NASA Langley Research Center, Hampton, VA 23681-2199, USA

ARTICLE INFO

Article history:
Received 18 February 2011
Received in revised form
24 March 2011
Accepted 27 March 2011
Available online 2 April 2011

Keywords:
Molecular dynamics
Crosslinking
Glass transition

ABSTRACT

Molecular dynamics and molecular mechanics simulations are used to establish well-equilibrated, validated molecular models of the EPON 862-DETDA epoxy system with a range of crosslink densities using a united atom force field. Molecular dynamics simulations are subsequently used to predict the glass transition temperature, thermal expansion coefficients, and elastic properties of each of the crosslinked systems. The results indicate that glass transition temperature and elastic properties increase with increasing levels of crosslink density and the thermal expansion coefficient decreases with crosslink density, both above and below the glass transition temperature. The results demonstrate reasonable agreement with thermomechanical properties in the literature. The results also indicate that there may be a range of crosslink densities in epoxy systems beyond which there are limited changes in thermomechanical properties.

1. Introduction

Epoxy-matrix composites are one of the primary structural materials used in modern civilian aircraft. Their popularity is due to their excellent specific stiffness, specific strength, and processing properties. Because the mechanical properties of epoxy composites depend significantly on the molecular-scale structure of these materials, structure–property relationships are needed to permit design optimization. This also applies to processing conditions, which can significantly alter the structure, and therefore properties, of epoxy composites.

Epoxy resins are formed when epoxy monomers react with compounds known as crosslinking or curing agents, with active hydrogens such as amines and anhydrides [1]. Trial-and-error approaches for experimentally optimizing the processing conditions of epoxy materials can become time-consuming and expensive. Over the last two decades, molecular dynamics (MD) simulations based on bead-spring models [2,3] and Monte-Carlo simulations based on the bond-fluctuation model [4–6] have been used to study the molecular behavior of epoxy materials. The bead-spring models do not fully consider the details of the molecular structures and thus cannot predict the influence of specific groups of atoms on the physical properties. In the last few years, MD at the atomic scale has been quite successful in exploring different phenomena occurring at pico- to nano-second time scales in epoxy resins [7]

Many researchers have studied the formation of crosslinked epoxy resins using different approaches of simulated crosslinking. Doherty et al. [8] created PMA networks using lattice-based simulations using polymerization molecular dynamics scheme. Yarovsky and Evans [9] discussed a crosslinking technique which they used to crosslink low molecular-weight, water-soluble, phosphate-modified epoxy resins (CYMEL 1158). The crosslinking reactions were carried out simultaneously (static crosslinking process). Crosslinking of epoxy resins using molecular dynamics was performed by Xu et al. [1] and their model was used to study the diffusion of water in crosslinked networks. An iterative Molecular Dynamics (MD)/Molecular Minimization (MM) procedure was used to crosslink an epoxy resin (DGEBA), with one crosslink established per iteration. Other computational studies [10,11] involving crosslinking of epoxies have been performed. All of the studies discussed thus far were performed on relatively small model systems (less than 2200 atoms).

Heine et al. [12] simulated large PDMS networks using a dynamic crosslinking approach and Varshney et al. [7] used

* Corresponding author.
E-mail address: gmodegar@mtu.edu (G.M. Odegard).

0032-3861/$ – see front matter © 2011 Elsevier Ltd. All rights reserved.
doi:10.1016/j.polymer.2011.03.052

Heine's dynamic crosslinking approach and Xu's MD/MM concept [1] to crosslink EPON 862 with DETDA. Varshney et al. [7] modeled two different systems having molecules of EPON 862 and DETDA in the ratios of 128:64 and 256:128 (EPON862:DETDA). Although these studies have made significant progress in the molecular modeling of crosslinked epoxies, relatively large molecular models (>20,000 atoms) have not yet been developed to predict the influence of crosslink density on a wide range of thermomechanical properties of EPON 862-DETDA polymers.

The objective of this study was to establish a relatively large molecular model of the EPON 862-DETDA crosslinked epoxy system and to predict the influence of crosslink density on the thermomechanical properties. In this paper, an efficient and accurate methodology of creating molecular models of a crosslinked epoxy system containing more than 25,000 atoms is described. Molecular models are built for three different crosslink densities, and the models predict that the glass transition temperature, coefficient of thermal expansion, and elastic properties are dependent on the crosslink density. The results also suggest that there may be a small range of crosslink density which exhibit insignificant changes in properties. The results of this paper are generally consistent with experimental data and computational data of similar studies. Deviations of the results with the literature are discussed.

2. Molecular modeling

This section details the procedure for establishing the molecular model of the crosslinked epoxy. The modeling of the uncrosslinked monomer/hardener solution is described first, followed by a description of the crosslinking procedure. The LAMMPS (Large Scale Atomic/Molecular Massively Parallel Simulator) software package [13] was used for all of the MM and MD simulations described herein.

2.1. EPON 862-DETDA uncrosslinked structure

The initial uncrosslinked molecular model structure was established using a procedure similar to that used by Varshney et al. [7] and consisted of the EPON 862 monomer (Di-glycidyl ether of Bisphenol-F) and the crosslinking agent DETDA (Diethylene Toluene Diamine). The molecules of EPON 862 and DETDA are shown in Fig. 1. A stoichiometric mixture of 2 molecules of EPON 862 and 1 molecule of DETDA was modeled first. The initial atomic coordinates were written to a coordinate file in the native LAMMPS format and the OPLS United Atom force field [14–16] was used for defining the bond, angle, and dihedral parameters. The OPLS United Atom force field was developed by Jorgensen and co-workers [14,15,17]. In this force field, the total energy of a molecular system is a sum of all the individual energies associated with bond, angle, dihedral, and 12-6 Lennard–Jones interactions. The equilibrium spacing parameter σ of the Lennard–Jones potential was taken to be the arithmetic mean of the individual parameters of the respective atom types while the well depth parameter ε was taken to be the geometric mean of the values of the respective atom types. The non-bonded van der Waals interactions were modeled using the 12-6 Lennard–Jones potential. By using this particular united atom force field, all CH_3, CH_2, CH, and alkyl groups were modeled as single united atoms with their corresponding masses, except for the C and H atoms in the phenyl rings of both the monomer and hardener molecules and one CH_3 group directly connected to the phenyl ring of the DETDA molecule. Thus in a 2:1 structure the number of atoms was reduced from 117 atoms to 83 atoms by the use of united atoms. As shown in Fig. 1, one molecule of EPON 862 has 31 atoms (including united atoms) and one molecule of DETDA has 21 atoms (also including united atoms).

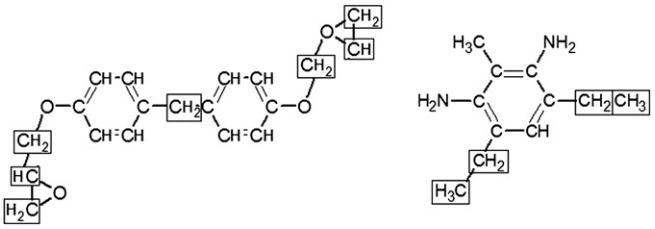

Fig. 1. Molecular structures of EPON 862 resin and DETDA crosslinking molecules. Atoms in boxes have been considered as united atoms.

The initial 2:1 structure was formed in a 10 × 10 × 10 Å simulation box with periodic boundary conditions. This structure was subjected to four MM minimizations and three MD simulations in order to minimize internal forces (thus reduce internal residual stresses) resulting from the construction of bonds, bond angles, and bond dihedrals. After stabilizing at a relatively low energy value, this structure was replicated to form eight more structures within the simulation box so that a 16:8 molecular mixture of EPON 862 and DETDA monomers was established. A slow stress relaxation procedure was performed over a cycle of 20 MM and 10 MD simulations. All MD simulations were conducted in the NVT (constant volume and temperature) ensemble for 100 ps at 600 K. The NVT ensemble made use of the Nose/Hoover thermostat and barostat for temperature and pressure control, respectively [18]. After every cycle of MD and MM, the box size was reduced by a small amount. After all MM and MD runs, a density of 1.21 g/cm^3 (1210 kg/m^3) was achieved. The final pressure value of the last minimization was less than 1 atm (101,325 Pa) which indicated that the structure had almost no residual stress. This equilibrated structure was used for the subsequent crosslinking step.

2.2. Crosslinking procedure

The equilibrated structure of the 16:8 model was statically crosslinked based on the root mean square (RMS) distance between the N atoms of DETDA and CH_2 groups of the EPON 862 molecules, similar to the approach used by Yarovsky and Evans [9]. Simultaneous breaking of CH_2–O bonds in the epoxide ends of the EPON 862 molecules and N–H bonds of the DETDA molecules made the activated CH_2 ends capable of forming crosslinks with activated N atoms of the DETDA molecules. A particular activated N could form a crosslink with the activated CH_2 of any adjacent EPON 862 molecule within a specified cutoff distance. While the actual crosslinking reaction is quite complex, the fundamental mechanisms that were modeled in this work are depicted in Figs. 2 and 3. Three assumptions were made for the crosslinking process:

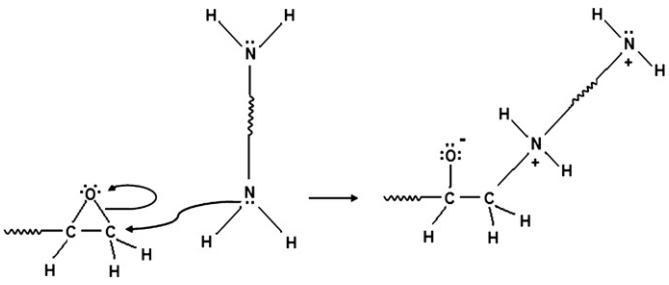

Fig. 2. First step of Crosslinking reaction: The lone pair of electrons of the nitrogen atom attacks the carbon atom next to the epoxide oxygen, forming a C–N bond and leaving a negative charge on the oxygen and a positive charge on the nitrogen. (The wavy lines represent the remaining parts of the EPON 862 and DETDA molecules in the respective structures).

1) Both primary amines in DETDA were assumed to have the same reactivity
2) The CH_2–O and N–H bonds were broken simultaneously (Fig. 2)
3) An N atom was partially activated when it had only one activated CH_2 within a defined cutoff distance.

The starting point of the crosslinking reaction is shown in Fig. 2 where the nucleophilic amine of the DETDA molecule reacts with the unsubstituted epoxy C, and the adjacent oxygen atom attains a negative charge when the C–O bond is broken. After forming a bond with the C atom, the N atom attains a positive charge and thus the neutrality of the EPON 862-DETDA system is maintained. Crosslinks were formed by computing all RMS distances between each N atom and the CH_2 united atoms within a defined cutoff distance. The CH_2 radicals located outside the cutoff distance of a particular NH_2 group were not crosslinked to that particular group. The cutoff distance was chosen to achieve a desired level of crosslinking as mentioned below. In the next step, the H ions were formed by breaking NH_2 bonds and were reacted with the O^- atoms of the broken epoxide ends. This bond formation was also performed based on the closest RMS distances between the O^- and H^+ atoms. The second step of the crosslinking reaction is shown in Fig. 3.

To determine the influence of the RMS distance on the total number of crosslinks formed, the crosslink density was determined for a range of RMS cutoffs for two different molecular models constructed in the manner described above (Fig. 4). The crosslink density of the epoxy system was defined as the ratio of the total number of crosslinks that were formed to the maximum number that could be formed. For example, an epoxy network having 16 out of 32 crosslinks is defined as having a 50% crosslink density.

In Fig. 4 a steep rise can be seen where the crosslink density increased from just above 15% to almost 60% over a span of a cutoff distance between 2 and 4 Å. Another important aspect of this graph is the plateau over which the crosslink density increased very little over a range of 4–8 Å and again after 10 Å. It is important to note that the trends of the two systems are very similar, demonstrating reproducibility in the crosslink density/RMS distance relationship. Therefore, a large increase in crosslink density occurred from 28% to 56% for the first system over a range difference of 1 Å. For the second system, the large increase in crosslink density occurred from 3% to 38% over 1 Å range. This trend was close to the trend of

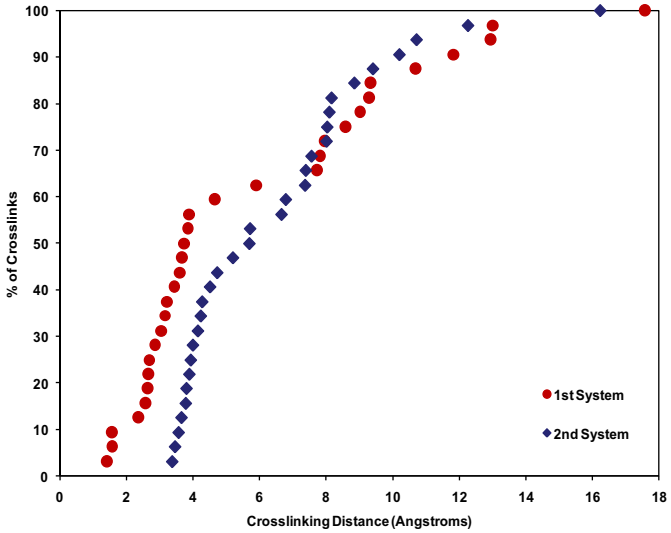

Fig. 4. The dependence of the crosslink density on crosslinking cutoff distance for two different crosslinked structures.

crosslink densities found by Varshney et al. [7] by using an alternative, dynamic-based crosslinking approach. Varshney et al. reported an increase in crosslink density from 0% to 80% over a range difference of 1 Å. This demonstrates that the extent of crosslinking increases rapidly over a certain range of distance between the crosslinking atoms.

Three representative crosslink densities were chosen for the subsequent modeling steps: 50% at a cutoff of 3.8 Å, 59% at a cutoff of 5 Å and 72% at a cutoff of 8 Å. These crosslink densities were chosen because they represent the expected range for a stoichiometric monomer/hardener mixing ratio.

2.3. Modeling EPON 862-DETDA structure having 432:216 stoichiometric ratio

The crosslinked 16:8 models were equilibrated by performing two MM minimizations and one MD run alternately to remove the residual stresses generated during the formation of the crosslinks. The MD runs were NVT simulations for 100 ps at 500 K. The

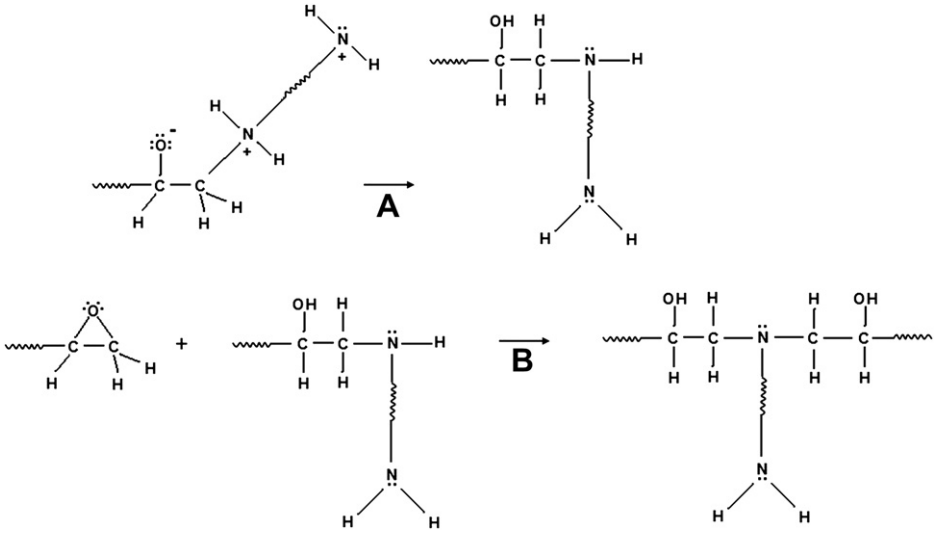

Fig. 3. Second and Final steps of crosslinking reaction: (A) The negatively charged oxygen abstracts a proton from the neighboring protonated amine, resulting in an alcohol group and an amine group and the crosslinking is complete. (B) The same crosslinked nitrogen reacts with another epoxide end of EPON 862 in the same way and forms two crosslinks.

equilibrated, crosslinked 16:8 models were replicated 26 times for each crosslink density, and each replica was rotated and translated to form a 3 × 3 × 3 array of 16:8 structures for each crosslink density. The large systems had 432 molecules of EPON 862 and 216 molecules of DETDA (Fig. 5). For three different defined crosslink densities, the 16:8 models had differences in the number of bonds, angles, and dihedrals. Each of these three samples had 17,928 united atoms representing a total 25,272 explicit atoms.

The models having a 432:216 monomer ratio of EPON 862 and DETDA chains were further equilibrated using MD and MM techniques with continuous shrinking of the volume until the models reached densities close to 1.2 g/cm^3(1200 kg/m^3). Between 30 and 35 minimizations and 12 NVT simulations were required for the equilibration of each individual 432:216 EPON 862-DETDA model. At every stage of volume reduction, one minimization was performed to relax the coordinates of the atoms in the new reduced size of the simulation box. This was followed by a 100 ps NVT simulation at 500 K. The temperature for NVT was kept relatively high so that atoms had enough kinetic energy to sample local configuration space. This was followed by one or two minimizations, depending on the energy and pressure values obtained after the simulations. That is, if the pressure was not close to 1 atm after the first minimization after the NVT simulation, then very small changes were made to the box dimensions and a subsequent minimization was performed. Once equilibrated, the models were further crosslinked based on RMS cutoff distance approach described above. The additional crosslinking steps were performed so that the 27 sub-units of the molecular model were crosslinked with one another, thus creating a stable solid structure and increasing the crosslink densities further. The 50% crosslinked structure had a 54% crosslink density after this step, the 59% crosslinked structure became 63% crosslinked and the 72% crosslinked structure increased to 76%. After this additional process of crosslinking, the structures were further equilibrated at the same volume with two NVT simulations at 500 K and 300 K for 100 ps each with in-between MM minimizations. It is important to note that the equilibrated structures model an infinite network of crosslinked epoxy due to the use of periodic boundary conditions. Therefore, the modeled structures do not represent localized crosslinking, which is observed in microgels with highly-crosslinked particles on the order of 10 Å [19]

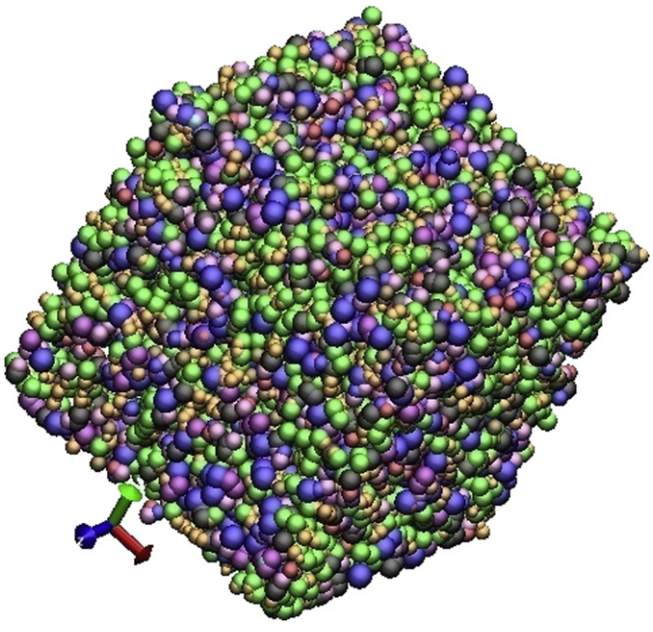

Fig. 5. 432:216 model of EPON 862-DETDA containing 17,928 united atoms.

The spatial density distributions of these structures were calculated to determine the degree of uniformity of the polymer in the simulation box. The simulation boxes for each crosslink density were equally divided into 10 divisions along the *X*, *Y* and *Z* axes and the total masses of all the atoms present in each of those ten divisions was determined. The total mass of atoms present in each division was then divided by the volume of that division to calculate the density of atoms present in that particular division. The spatial density distributions of the 54%, 63% and 76% crosslinked systems are shown in Fig. 6.

The data in Fig. 6 indicate that the densities of the 54%, 63%, and 76% crosslinked systems were uniform along all three axes of the simulation boxes. This indicated that the equilibration method involving minimizations and in-between NVT simulations was thorough and led to a homogeneous epoxy network.

3. Results and Discussions

Once models were equilibrated, they were used to determine the glass transition temperature (T_g), thermal expansion coefficient, and elastic properties of each of the crosslinked systems. The procedures and results for these simulations are described in this section.

3.1. Glass transition temperature range determination

For each of the three crosslinked epoxy models, NPH (constant pressure and constant enthalpy) simulations were run for 400 ps from −70 °C (203 K) to 330 °C (603 K) at pressures of 1 atm. These simulations were performed to simulate the process of constant heating of the epoxy systems from cryogenic temperatures to elevated temperatures. Using the results of the NPH simulations, density versus temperature curves were plotted which are shown in Fig. 7 for the 54%, 63% and 76% crosslinked systems. Data within the temperature range of −30 °C to 300 °C was used for calculating glass transition temperatures. The simulation data within the initial temperature range from −70 °C to −30 °C were discarded to eliminate the effects of molecular relaxation and initial oscillation of the temperature and pressure around the set values. The density–temperature curves showed a characteristic change in slope in the T_g region. Typically the T_g is determined by finding the intersection between linear regression lines fit to the data points below and above the change in slope. However, the change in slope is usually gradual. As a result, the T_g determination is highly sensitive to the manner in which the data points on the density versus temperature graph are fit. Therefore, it is more appropriate to describe the T_g as a temperature range rather than a single temperature value. To determine the T_g range, a series of linear regression lines were fit using temperature ranges of 80°, 90°, 100°, 110° and 120° C intervals of temperature for each of the crosslinked systems shown in Fig. 7. The ranges of the intersection points from these series of fits comprised the T_g range.

The T_g was found to be in the range of 124 °C–141 °C with an average T_g of 133.44 °C for the 54% crosslinked structure. For the 63% crosslinked structure, an average T_g of 142.10 °C was found in the range of 132 °C–149 °C. For the 76% crosslinked structure, an average T_g of 151.20 °C was found in the range of 143 °C–157 °C. From the data it is clear that the average T_g increased as the crosslink density increased, which is likely due to the increasing number of covalent bonds as the crosslink density increases. As a result, there is more resistance to increases in free volume as the temperature increases for increased levels of crosslinking. Similar increases in T_g due to additional crosslinking have been observed in graphite–epoxy composites [20,21]

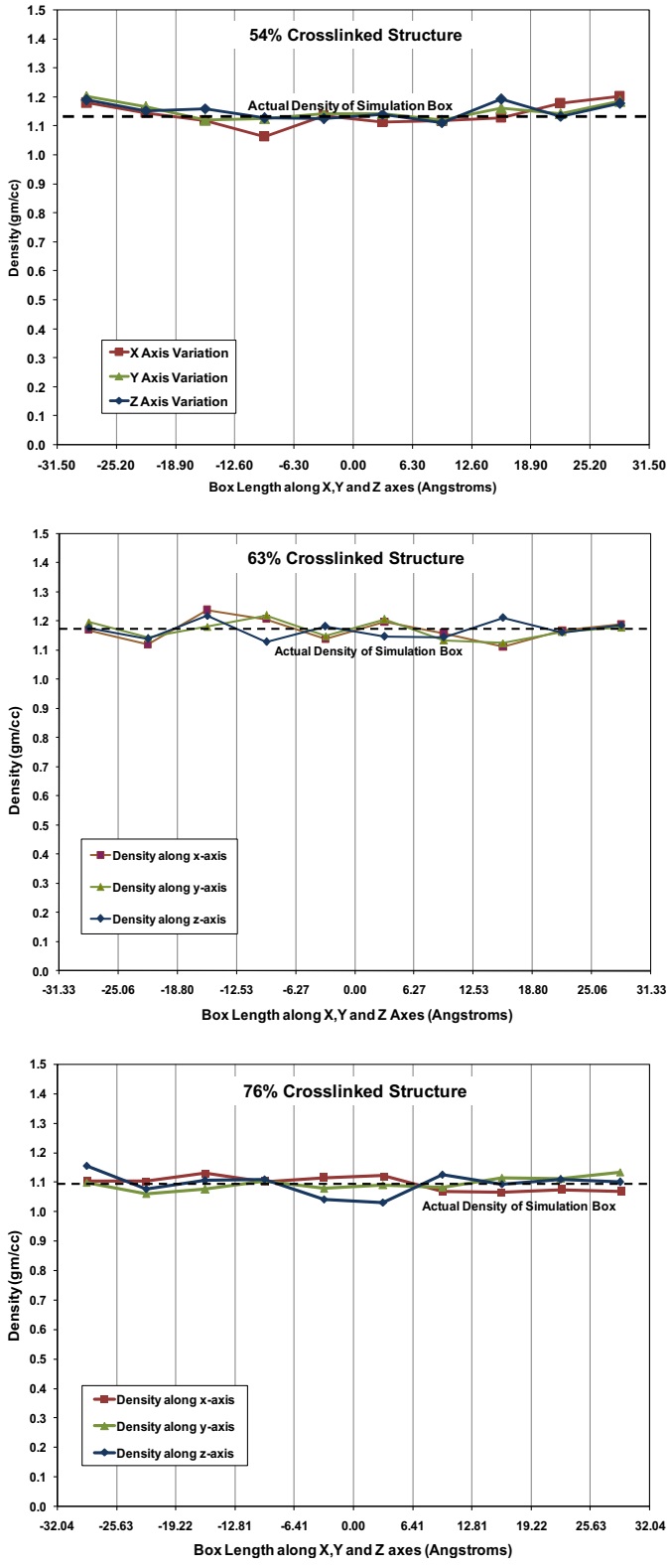

Fig. 6. Spatial Density distributions of 54%, 63% and 76% crosslinked structures along the length of simulation box.

In Fig. 7, the density of the 54% crosslinked system is lower than that of the 76% crosslinked system at high temperatures, while this trend is opposite at lower temperatures. The reason for this behavior can also be explained based on the difference in crosslink density. 54% crosslinked structure had more uncrosslinked freely-moving polymer chains that reoriented themselves into a dense configuration at lower temperatures. At high temperatures, the uncrosslinked epoxy chains can lead to more expansion of the volume and thus the 54% crosslinked structure had a lower density than the 76% crosslinked structure. All these NPH simulations were performed by using equilibrated configurations of these crosslinked systems. During equilibration, volumes of the crosslinked structures were decreased based on two criteria: 1. The pressure has to decrease along with the energy during a minimization 2. The final equilibration should lead to a pressure of close to 1 atm with the structure attaining a density of around 1.2 g/cm^3

The equilibration process of the 63% crosslinked structure made its density slightly higher than the densities of the equilibrated 54% and 76% crosslinked structures. As the density was already a bit high before the NPH simulations were started, the 63% crosslinked structure's density varied over a range which did not overlap the density variations of the other two systems. In this research, the focus was placed on the variations of the densities with respect to temperature, not on the absolute value of the densities. This issue would likely be resolved if multiple material systems were independently constructed for each crosslink density. Because of limited computational recourses, only one structure was established for each crosslink density for the current study.

Varshney et al. [7] predicted a T_g of 105 °C for the same EPON 862-DETDA system but with a crosslink density of 95%. Fan et al. [10] predicted the T_g for a 100% crosslinked EPON 862-DETDA system to be 109 °C. Miller et al. [22] experimentally measured a T_g of 150 °C for the same epoxy system, though the actual crosslink density was unknown. Clearly, the presently predicted values of all three crosslinked systems agree with the experimental values more than they agree with the predicted values in the computational literature. Both Varshney et al.'s work and Fan et al.'s work have predicted T_g values much less than experimentally measured values. This is especially surprising since the simulated cooling rates are much faster than the experimental cooling rate, which should lead to higher predicted values of T_g. The predicted values in the current study do not show such a discrepancy with experiment, which indicates that the chosen OPLS force field, equilibration process, and simulated heating process accurately modeled the molecular behavior of the epoxy system.

3.2. Volume shrinkage and thermal expansion coefficients

Using the results from the NPH simulations described in the previous sub-section, the volume shrinkages with respect to the volume at 300 °C for the 54%, 63%, and 76% crosslinked systems for the temperature range of −30 °C to 300 °C were determined and are plotted in Fig. 8. From the plot it is clear that all three systems experienced significant changes in volume when heated to elevated temperatures. It is also clear that the 54% crosslinked system exhibited a significantly larger amount of shrinkage than the 63% and 76% systems, which were nearly identical. This is likely due to the difference in the number of covalent bonds present in the three structures. The 54% crosslinked structure had fewer covalent bonds and a larger number of free chains with higher mobility than the 63% and 76% crosslinked structures. Therefore, at decreasing temperatures, the 54% crosslinked model was able to adapt a more compact conformation than the 63% and 76% crosslinked models.

Linear regression lines were fitted on the volume shrinkage curves shown in Fig. 8 to determine the coefficient of volumetric thermal expansion (CVTE) in both the rubbery and glassy regimes. Because the method of fitting the data can affect the resulting predicted values of CVTE (similar to the predicted T_g described above), two different ranges were chosen to fit the curves for both the rubbery and glassy regions. In the glassy regime, the data were

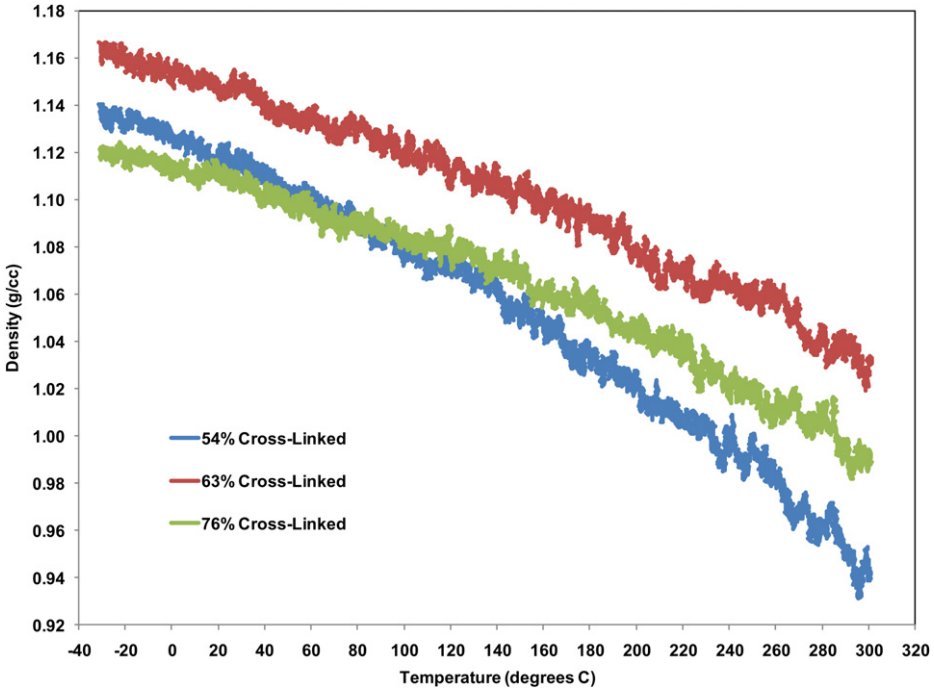

Fig. 7. Density vs. temperature curves for 54%, 63% and 76% crosslinked system.

fit for the 0°–120 °C range and the 20°–120 °C degree range. For the rubbery region, ranges of 160°–280 °C degrees and 160°–260 °C degrees were fit. Therefore, temperature ranges of 100° and 120 °C were fit above and below the T_g, and the CVTE was calculated with

$$\beta = \frac{1}{V_0}\left(\frac{\partial V}{\partial T}\right)_P \tag{1}$$

where V_0 is the initial volume of the simulation box before the NPT simulation, and the subscript P implies a constant-pressure process. The coefficient of linear thermal expansion (CLTE) is defined as

$$\alpha = \frac{\beta}{3} = \frac{1}{L_0}\left(\frac{\partial L}{\partial T}\right)_P \tag{2}$$

where L_0 is the initial length of each side of the cubic simulation box before the NPH simulation. The CLTE values obtained for the three

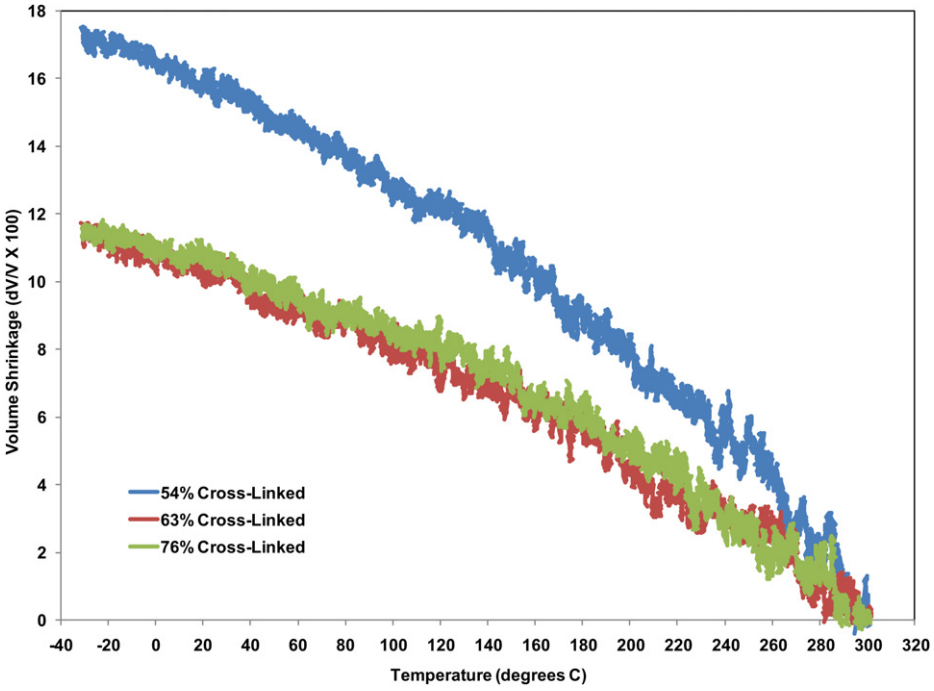

Fig. 8. Volume shrinkages with respect to the volume at 300 °C for 54%, 63% and 76% crosslinked structures.

crosslinked systems are given in Table 1. These values are the averages of the CLTE values obtained over the temperature ranges of 100° and 120 °C.

The results shown in Table 1 generally indicate an increasing trend in the coefficients of expansion with decreasing crosslink density, which is likely because the polymer chains are less constrained in lower-crosslink systems, resulting in greater mobility during the thermal expansion process. This also explains the greater expansion that was predicted above T_g for each of the crosslink densities. The results were found to be consistent with those reported by Fan et al. [10] and Wang et al. [23]. Fan et al. predicted CLTE values of $18.5 \times 10^{-5\circ}C^{-1}$ above T_g and $5.5 \times 10^{-5\circ}C^{-1}$ below T_g for a 100% crosslinked EPON 862-DETDA system. Wang et al's experimental work with the pure EPON 862-DETDA system gave CLTE values of $18 \times 10^{-5\circ}C^{-1}$ above T_g and $6.4 \times 10^{-5\circ}C^{-1}$ below T_g.

3.3. Elastic properties

Simulated deformations were performed on all three crosslinked systems to determine their elastic properties. In these simulations, strains were imposed on the periodic MD models in the NVT ensemble, and the corresponding averaged stress components (virial stress) were determined for a complete stress–strain response. Two types of strains were applied on the structures: volumetric and three-dimensional shear strains. NVT simulations were run at 300 K (room temperature) for 200 ps with timesteps of 0.2 fs. Strain increments were applied at every timestep such that the desired cumulative strain was reached by the end of the 200 ps simulation. It is important to note that although the elastic response of polymers is generally dependent on applied strain rate, and the simulated deformations are at relatively high-strain rates, it is expected that the predicted elastic properties are close to those observed experimentally. Although excellent agreement between experiment and high-strain rate simulations has been observed in the literature [24–26], the reason for the apparent lack of strain-rate effects in predicted properties is unclear. For the volumetric strains, equal strain magnitudes were applied in all three coordinate directions in both tension and compression according to kinematic equation

$$\varepsilon_{xx} = \varepsilon_{yy} = \varepsilon_{zz} = \pm 0.005 \tag{3}$$

where ε_{ij} is the infinitesimal strain tensor component with respect to coordinate directions i and j. The overall dilation of the molecular model was

$$\Delta = \varepsilon_{xx} + \varepsilon_{yy} + \varepsilon_{zz} \tag{4}$$

For each timestep in these simulations, the overall hydrostatic stress σ_h of the model was calculated by

$$\sigma_h = \frac{1}{3}(\sigma_{xx} + \sigma_{yy} + \sigma_{zz}) \tag{5}$$

where σ_{ij} is the volume-averaged viral stress tensor component with respect to the coordinate directions i and j. For each timestep of the final 198 ps of the simulations, the hydrostatic stress and dilatation were used to perform a linear regression analysis to establish the bulk modulus

$$K = \frac{\sigma_h}{\Delta} \tag{6}$$

The bulk moduli calculated for positive and negative dilatations were averaged. The data gathered during the first 2 ps of the simulations were not used in the regression analysis because molecular structures typically undergo rapid, local relaxation during the initial stages of MD simulation. The structures were well-equilibrated before the start of these deformations and thus did not need significant time for relaxation. In the initial 1–1.5 ps of the deformation simulation, the initial oscillation of the total pressure values died out. Nearly one million data points were used to calculate the bulk modulus for each epoxy system. Similarly, a three-dimensional shear strain was applied to the molecular models

$$\gamma_{xy} = \gamma_{yz} = \gamma_{zx} = \pm 0.005 \tag{7}$$

where γ_{ij} is the infinitesimal engineering shear strain component with respect to the i and j coordinate directions. The corresponding volume-averaged shear stresses σ_{yz}, σ_{xz}, and σ_{xy} were calculated for each timestep. Each shear stress component was compared to the corresponding applied shear strain for each timestep of the final 198 ps of the simulations. A linear regression analysis was performed to determine the corresponding shear modulus, which is given by

$$G = \frac{\sigma_{xy}}{\gamma_{xy}} \tag{8}$$

For each crosslink density, the three calculated shear moduli were averaged for both positive and negative applied shear strains. After calculating bulk moduli and shear moduli for all the crosslinked structures, Young's moduli (E) and Poisson's ratios (ν) were calculated according to

$$E = \frac{9KG}{3K + G} \tag{9}$$

$$\upsilon = \frac{3K - 2G}{2(3K + G)} \tag{10}$$

Using Equations (3)–(10), the elastic properties were calculated for the 54%, 63% and 76% crosslinked structures and the values are given in Table 2.

The results in Table 2 show an increasing trend in Young's modulus and shear modulus among the 54%, 63% and 76% crosslinked structures. Littell et al. [27] experimentally measured mechanical properties of the same epoxy system and reported Young's modulus values of 1.6–2.9 GPa, shear modulus Values of 0.6–1.0 GPa, and Poisson's ratio in the range of 0.35–0.43. Fan et al. [10] predicted Young's modulus of 3.75 GPa for their 100% crosslinked EPON-DETDA computational model. The results obtained in this computational study are thus consistent with the literature [10,27].

The bulk modulus shows a very small decreasing trend with increasing crosslink density, signifying that volumetric deformation

Table 1
Thermal Expansion Coefficients of crosslinked structures.

Coefficient of Linear Thermal Expansion (α) $\times 10^{-5}$ ($^\circ C^{-1}$)			
	54%	63%	76%
Above T_g	20.0	13.6	14.0
Below T_g	12.9	9.1	8.6

Table 2
Mechanical properties of crosslinked structures (units in GPa).

	K (bulk modulus)	G (shear modulus)	E (Young's modulus)	υ (Poisson's ratio)
54% Crosslinked	2.961	0.154	0.453	0.475
63% Crosslinked	2.914	0.707	1.963	0.388
76% Crosslinked	2.661	0.831	2.258	0.359
Experimental sample [27]		0.6–1.0	1.6–2.9	0.35–0.43

probably does not have a strong sensitivity to crosslinking. The increasing trends in shear modulus and Young's modulus with increasing crosslink density indicate that with crosslinking, the molecular structure becomes stiffer because of the presence of more covalent bonds. Similar trends have been reported in other epoxy systems by Gupta et al. [28] and in epoxy-nanotube composites by Miyagawa et al. [29]. Lees and Davidson [30], Lee and Neville [31], and Burhans et al. [32] discuss data that show increasing distances between reactive sites in epoxies result in decreasing crosslink densities and decreasing elastic properties. It is important to note that this trend is not always observed, specifically, Vakil and Martin [33] reported that glassy modulus is not affected by the degree of crosslinking. Another important observation is the similarity of shear modulus, Young's modulus, and Poisson's ratio values of the 63% and 76% crosslinked structures. This similarity in mechanical properties is in agreement with the volume shrinkage results discussed above. It is important to note that these results may be sensitive to the limited number of modeled systems at each crosslink density. That is, if multiple systems had been individually constructed at each crosslink density, the apparent trends could differ slightly. Because of the uniform distribution of density and the agreement between computed and measured T_g values (described above), the trends in elastic moduli should be accurately reflected in the modeled molecular structures. Furthermore, it is important to note that although the predicted elastic properties are intuitive, that is, the elastic moduli are the same magnitude as the majority of polymers (Young's modulus between 1 and 5 GPa), the importance of the results is in the model validation and predicted trends as a function of crosslink density and the ability to predict this trend computationally.

4. Conclusions

A molecular modeling study of a crosslinked EPON 862-DETDA epoxy polymer with various degrees of crosslinking has been performed using a united atom force field. The T_g, thermal expansion coefficients, and elastic properties of the epoxy system were predicted for a range of crosslink densities. The predicted thermomechanical properties were mostly consistent with those given in literature, thus validating the computational approach used. The results indicate that with increasing crosslink density, the T_g and elastic stiffness tend to increase, while the coefficient of thermal expansion decreases, both above and below T_g. For thermal expansion coefficients and elastic properties, the magnitude of these changes generally decreased substantially for crosslink densities above 63%.

The density versus temperature curves that were used to determine the T_g of the simulated epoxy indicate that reporting singular values of T_g may be unrealistic for models of the size mentioned in this work. The nonlinearity in these curves introduces a degree of subjectivity for the determination of T_g using regression analyses above and below the nonlinear portion of the curves. Instead, the T_g should be reported as a temperature range in which the physical structure of the polymer undergoes a structural change.

The results of this study also indicate that for this epoxy system, and possibly similar epoxy systems, there might be a threshold crosslink density beyond which thermomechanical properties exhibit little change. At 63% crosslinking, the structure is already immobilized to a large extent and increasing the crosslink density to 76% may only change the thermomechanical properties slightly. Unfortunately, it is difficult to experimentally quantify the crosslink density of epoxies. The extent of cure can be monitored during the polymerization reaction using Infrared (IR) or dielectric spectroscopy. These techniques utilize changes in spectral features, such as the intensity of the epoxide group vibration (IR) [34,35] or the frequency of maximum permittivity or loss (dielectric) [36,37], to determine the progress of reaction. So while these methods permit the study of the cure reaction and yield a relative measure of the extent of reaction, they cannot determine the crosslink density for a cured epoxy sample. Without this data, it is difficult to make definitive statements regarding the validation of the observations in this study.

Acknowledgments

This research was funded by NASA under the Aircraft Aging and Durability Project (Grant NNX07AU58A) and by the Air Force Office of Scientific Research under the Low Density Materials Program (Grant FA9550-09-1-0375). We thank Dr. Sarah Jane Frankland of National Institute of Aerospace (NIA), Dr. Jeffrey Hinkley of NASA, and Dr. Steve Plimpton of Sandia National Laboratories for their vital suggestions.

References

[1] Wu CF, Xu WJ. Polymer 2006;47(16):6004–9.
[2] Stevens MJ. Macromolecules 2001;34(8):2710–8.
[3] Tsige M, Stevens MJ. Macromolecules 2004;37(2):630–7.
[4] Carmesin I, Kremer K. Macromolecules 1988;21(9):2819–23.
[5] Jo WH, Ko MB. Macromolecules 1994;27(26):7815–24.
[6] Jo WH, Ko MB. Macromolecules 1993;26(20):5473–8.
[7] Varshney V, Patnaik SS, Roy AK, Farmer BL. Macromolecules 2008;41(18):6837–42.
[8] Doherty DC, Holmes BN, Leung P, Ross RB. Computational and Theoretical Polymer Science 1998;8(1–2):169–78.
[9] Yarovsky I, Evans E. Polymer 2002;43(3):963–9.
[10] Fan HB, Yuen MMF. Polymer 2007;48(7):2174–8.
[11] Fan HB, Chan EKL, Wong CKY, Yuen MMF. Journal of Electronic Packaging 2007;129(1):35–40.
[12] Heine DR, Grest GS, Lorenz CD, Tsige M, Stevens MJ. Macromolecules 2004;37(10):3857–64.
[13] Plimpton S. Journal of Computational Physics 1995;117(1):1–19.
[14] Jorgensen WL, Maxwell DS, TiradoRives J. Journal of the American Chemical Society 1996;118(45):11225–36.
[15] Weiner SJ, Kollman PA, Case DA, Singh UC, Ghio C, Alagona G, et al. Journal of the American Chemical Society 1984;106(3):765–84.
[16] Watkins EK, Jorgensen WL. Journal of Physical Chemistry A 2001;105(16):4118–25.
[17] Duffy EM, Kowalczyk PJ, Jorgensen WL. Journal of the American Chemical Society 1993;115(20):9271–5.
[18] Hoover WG. Physical Review A 1985;31(3):1695–7.
[19] Vanlandingham MR, Eduljee RF, Gillespie JW. Journal of Applied Polymer Science 1999;71(5):699–712.
[20] Mijovic J. Journal of Composite Materials 1985;19(2):178–91.
[21] Lee A, Mckenna GB. Polymer 1988;29(10):1812–7.
[22] Miller SRGD, Bail JL, Kohlman LW, Binienda WK. Effects of hygrothermal cycling on the chemical, thermal, and mechanical properties of 862/W epoxy resin. Austin, TX: Aircraft Airworthiness and Sustainment Conference; 2010.
[23] Wang SR, Liang ZY, Gonnet P, Liao YH, Wang B, Zhang C. Advanced Functional Materials 2007;17(1):87–92.
[24] Frankland SJV, Harik VM, Odegard GM, Brenner DW, Gates TS. Composites Science and Technology 2003;63(11):1655–61.
[25] Clancy TC, Frankland SJV, Hinkley JA, Gates TS. Polymer 2009;50(12):2736–42.
[26] Raaska T, Niemela S, Sundholm F. Macromolecules 1994;27(20):5751–7.
[27] Littell JD, Ruggeri CR, Goldberg RK, Roberts GD, Arnold WA, Binienda WK. Journal of Aerospace Engineering 2008;21(3):162–73.
[28] Gupta VB, Drzal LT, Lee CYC, Rich MJ. Polymer Engineering and Science 1985;25(13):812–23.
[29] Miyagawa H, Drzal LT. Polymer 2004;45(15):5163–70.
[30] Lees S, Davidson CL. Journal of Biomechanics 1977;10(8):473–86.
[31] Lee H, Neville K. Handbook of epoxy resins. New York: McGraw-Hill; 1967. 18–19.
[32] Burhans S, Pitt CF, Sellers RF, Smith SG. High performance epoxy resin systems for fiber-reinforced composites- preliminary paper. 21st Annual Meeting of the Reinforced Plastics Division, Society of Plastic Industry; 1965.
[33] Vakil UM, Martin GC. Journal of Applied Polymer Science 1992;46(12):2089–99.
[34] Acitelli A, Sacher E. Polymer 1971;12(5):335–43.
[35] Plazek DJ, Frund ZN. Journal of Polymer Science Part B-Polymer Physics 1990;28(4):431–48.
[36] Fitz BD, Mijovic J. Macromolecules 1999;32(12):4134–40.
[37] Levita G, Livi A, Rolla PA, Culicchi C. Journal of Polymer Science Part B-Polymer Physics 1996;34(16):2731–7.